

## Strain-dependent optical emission in $\text{In}_{1-x}\text{Ga}_x\text{As}/\text{InP}$ quantum wells

H. A. P. Tudury, M. K. K. Nakaema, and F. Iikawa

*Instituto de Física “Gleb Wataghin,” Universidade Estadual de Campinas, CP 6165, 13083-970 Campinas-SP, Brazil*

J. A. Brum

*Instituto de Física “Gleb Wataghin, Universidade Estadual de Campinas, CP 6165, 13083-970 Campinas-SP, Brazil  
and ABTLuS-Laboratório Nacional de Luz Síncrotron, CP 6192, 13083-061 Campinas-SP, Brazil*

E. Ribeiro, W. Carvalho, Jr., A. A. Bernussi, and A. L. Gobbi

*Laboratório Nacional de Luz Síncrotron-ABTLuS, CP 6192, 13083-061 Campinas-SP, Brazil*

(Received 31 May 2001; published 14 September 2001)

InGaAs/InP strained-layer modulation-doped quantum wells were studied by photoluminescence. The combination of the built-in strain and the quantum confinement in this system leads to a strong valence band mixing yielding direct and indirect band gap structures. We demonstrate that the optical emission line shape is strongly dependent on the valence band dispersion and it is a good method to distinguish between direct and indirect structures. The application of an external biaxial tensile strain to the samples provides an additional evidence of direct-to-indirect band gap transition in strained heterostructures.

DOI: 10.1103/PhysRevB.64.153301

PACS number(s): 78.66.Fd, 78.55.Cr, 78.30.Fs

### I. INTRODUCTION

Strained  $\text{In}_{1-x}\text{Ga}_x\text{As}/\text{InP}$  heterostructures grown on InP substrates are very suitable materials for band gap engineering and device applications.<sup>1-11</sup> InGaAs alloy layers can be grown under either a tensile or a compressive biaxial strain by changing the Ga content. Here we consider an  $\text{In}_{1-x}\text{Ga}_x\text{As}/\text{InP}$  quantum well (QW) where the  $\text{In}_{1-x}\text{Ga}_x\text{As}$  is the well material. The QW confinement breaks the valence band center-of-zone degeneracy and the top valence level is heavy-hole-like. For the QW width considered here, the next level is light-hole-like. In addition, the heavy-hole and the light-hole subbands shift towards (opposite to) each other when the InGaAs layer is under tensile (compressive) strain. By carefully tailoring the sample parameters such as the well width and the Ga concentration ( $x$ ) in the  $\text{In}_{1-x}\text{Ga}_x\text{As}$  alloy, one may reach a condition of indirect band gap energy structure. The designed band gap flexibility of the InGaAs system enables one to control the photocreated carrier radiative lifetime. Indirect band gap transition in InGaAs/InP heterostructure has been theoretically predicted<sup>4,5,7</sup> and experimental evidence has been reported for undoped samples.<sup>6</sup>

In this work, we present an optical study of the valence band structure of strained-layer InGaAs/InP  $n$ -type modulation-doped QW's. By varying the Ga concentration, the biaxial tensile strain in the QW layer can be increased leading to drastic changes in the band structure of this system, mainly in the valence band dispersion. Due to the presence of a high-density two-dimensional electron gas (2DEG) in the studied samples, the electron-hole pair recombination is governed by the photocreated hole distribution in  $k$  space. InGaAs/InP heterostructures allow us to optically study the evolution of the valence band structure from a direct-gap to an indirect-gap configuration. The calculated optical spectra evolution of modulation doped InGaAs/InP QW's as a function of biaxial tensile strain qualitatively agrees with the observed experimental results. We also demonstrate that an ex-

ternal biaxial tensile stress applied to a direct-gap sample induces a direct-to-indirect crossover. This behavior is equivalent to the one obtained by increasing the Ga concentration in the InGaAs/InP QW samples. The external strain applied to the QW's represents an alternative method to control the carrier radiative lifetime and the valence band effective mass in this system.

### II. EXPERIMENTAL DETAILS

The samples were grown by low-pressure metal-organic chemical vapor deposition (LP-MOCVD) on (001) InP:S substrates. The structure of the investigated samples consists of an InP buffer layer (1.9  $\mu\text{m}$  thick), a lattice-matched  $\text{In}_{0.53}\text{Ga}_{0.47}\text{As}$  (3.8  $\mu\text{m}$  thick), a 10 nm thick InP, a 10 nm thick Si-doped InP, a 10 nm thick InP, a 6 nm thick  $\text{In}_{1-x}\text{Ga}_x\text{As}$  QW, a 10 nm thick InP, a 10 nm thick Si-doped InP, and a 30 nm thick InP capping layer. The doped InP layers ( $N_{\text{Si}}=10^{18} \text{ cm}^{-3}$ ) are responsible for the formation of the 2DEG in the QW, with an electron density of  $n_s=5 \times 10^{11} \text{ cm}^{-2}$ .<sup>11</sup> We have studied a set of five samples with Ga concentration varying from 0.47 (direct gap) to 0.60 (indirect gap).

Photoluminescence (PL) experiments were performed using the 632.8 nm line of a He-Ne laser as the excitation source. The optical emission was detected by a cooled Ge photodiode coupled to a 0.5 m single spectrometer. The biaxial tensile strain was externally applied to the samples by a specially designed low-temperature pressure cell. All measurements were carried out at 2 K temperature (liquid He immersion cryostat).

### III. RESULTS IN DISCUSSIONS

Figure 1 shows the PL spectra of five samples with different Ga concentration. The peak position of the emission line shifts to higher energies as the Ga concentration in the

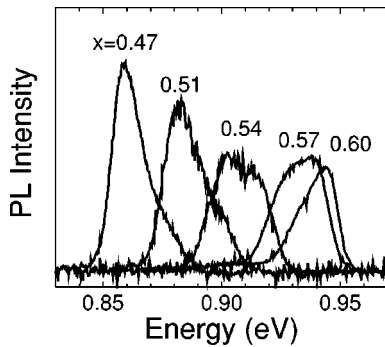


FIG. 1. Photoluminescence spectra of samples with different Ga composition.

$\text{In}_{1-x}\text{Ga}_x\text{As}$  alloy QW increases. This shift is a combination of two different effects. The dominant contribution comes from the increase of the gap energy of  $\text{In}_{1-x}\text{Ga}_x\text{As}$  alloy with  $x$ . The built-in biaxial tensile strain also increases with  $x$  (due to the increasing lattice mismatch relative to the InP barriers). However, it acts in the opposite direction, lowering the band gap energy. Although the strain has little effect on the net energy shift, it also changes the relative separation between the bands, which leads to strong modifications of the valence band dispersion.

The most remarkable feature shown in Fig. 1 is the dramatic evolution of the PL line shape as the Ga content is increased. This behavior can be qualitatively explained by using the schematic illustration shown in Fig. 2. Since the electron energy states are filled up to the Fermi energy, the line shapes of the optical transitions are determined by the photocreated hole distribution. After been created, these carriers relax their energy and momentum and occupy the top of the valence band. For direct-gap samples the holes are distributed around  $k=0$  and the recombination takes place close to  $E_0$  (effective gap energy), but broadened to higher energies (the hole population decreases with increasing  $k$ ). The high-energy tail of the PL spectrum is, therefore, related to the hole quasitemperature, which is assumed to be the sample temperature. The samples with  $x=0.47$  and  $0.51$  (see Fig. 1), which are expected to exhibit direct interband transitions, have a PL line shape consistent with this description. As the Ga concentration increases the hole effective mass

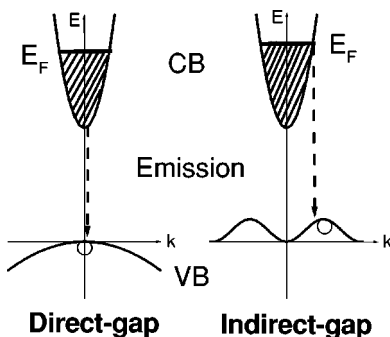


FIG. 2. Schematic illustration of the optical transitions in direct and indirect band structures in the presence of a two dimensional electron gas.

becomes heavier, allowing the holes to be distributed over a larger range of  $k$  values which broadens the optical transition due to the electron-hole recombination at different  $k$ 's. This interpretation also agrees with the fact that the PL line width of the sample with  $x=0.51$  is broader than the one with  $x=0.47$ . Following this tendency, by further increasing the Ga content, the valence band reaches the direct-to-indirect gap transition, exhibiting an almost flat energy band dispersion. In this case, the holes are distributed over an even larger range of  $k$  values, allowing for optical transitions from  $k=0$  to  $k_F$ . The net result is an almost squarelike PL line shape, as shown in the PL spectrum of the sample with  $x=0.54$  in Fig. 1. For higher  $x$ , the top of the valence band shifts to  $k_0 \neq 0$ , thus leading to an indirect band structure, allowing distribution of the photocreated holes over  $k$  around  $k_0$ , where  $k_0$  is the wave vector at the top of the valence band. The hole occupation decreases as the  $k$  value tends to zero and for  $k > k_0$ . Since there are electrons available for recombination from zero to  $k_F$ , and  $k_F$  is smaller than  $k_0$  (see below), the PL intensity is higher at  $k \sim k_F$ . The PL emission intensity decreases with decreasing  $k$ . In this case, the PL emission must exhibit a peak around the Fermi energy and a tail towards the low-energy side of the spectrum. This behavior can be clearly observed in the PL spectra of the samples with  $x=0.57$  and  $x=0.60$  in Fig. 1.

In order to verify the interpretation discussed above we calculated the valence band structure of our samples using the six-bands  $\vec{k} \cdot \vec{p}$  method,<sup>4,5,7,12</sup> including the heavy, light, and split-off hole bands. In addition to the strain effects, we also included the self-consistent potential from the 2DEG. Due to the narrowness of the QW this effect is small and it was neglected afterwards. The conduction band is assumed parabolic. The photoluminescence is calculated directly using the Fermi golden rule<sup>13</sup> and assuming that the photocreated carriers are thermalized to the lattice temperature. This is a reasonable assumption since the “intrinsic” 2DEG (originated from modulation doping) and the photocreated carriers reach a common temperature through electron-electron and electron-hole interaction. The experiments are performed under low excitation intensity and the photocreated carrier concentration is an order of magnitude lower than the “intrinsic” 2DEG. We used a Fermi-Dirac distribution function for carrier occupations in their respective bands. Figure 3(a) shows the calculated valence subband dispersion for InGaAs/InP heterostructures with different Ga concentration. It is clearly evident from this figure that as the Ga content increases the separation between the first heavy-hole and light-hole subbands decreases due to the increasing biaxial strain, leading to the crossover of the bands that is responsible for the direct-to-indirect gap transition. For both  $x=0.57$  and  $0.60$  the top of the indirect valence band is located at  $k_0 \sim 0.04 \text{ \AA}^{-1}$ , which is larger than  $k_F \sim 0.02 \text{ \AA}^{-1}$  (electron gas density  $\sim 5 \times 10^{11} \text{ cm}^{-2}$ ), so that these calculations support the interpretation of the PL line shapes given above. Figure 3(b) shows the calculated PL spectra for the same Ga content values of QW's as in Fig. 3(a). The calculated PL line shapes are in good qualitative agreement with the experimental results shown in Fig. 1.

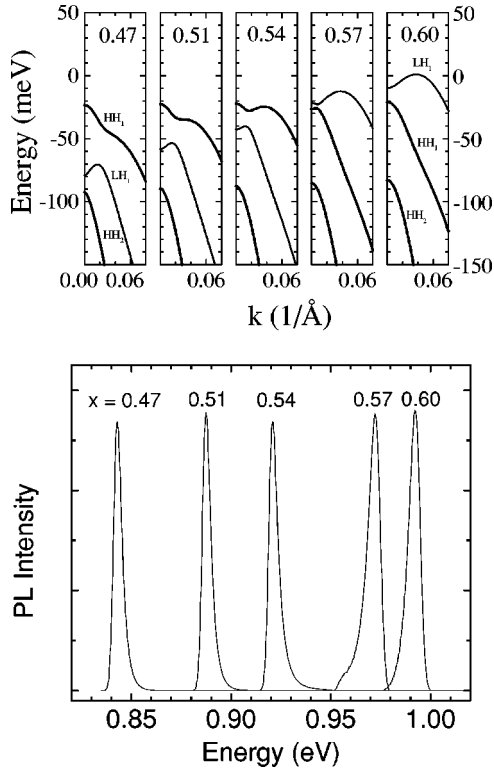


FIG. 3. (a) Valence band dispersion in InGaAs/InP QW's for Ga composition  $x=0.47, 0.51, 0.54, 0.57,$  and  $0.60$ . (b) Normalized calculated optical emission of InGaAs/InP QW's for the same Ga concentrations.

Direct-gap quantum wells have a peak around the band gap and a tail at the high-energy side. In contrast, indirect-gap samples show a low-energy side tail and a PL emission peak close to the Fermi energy. The theoretical PL spectra shown in Fig. 3(b) is sharper than those observed experimentally (Fig. 1). This difference is attributed to other physical mechanisms involved in optical emission, which are not included in our calculation, such as phonon-assisted emission, many-body effects, and particularly carrier localization effects. InGaAs/InP systems present strong inhomogeneous broadening due to the disorder of the ternary alloy, interface fluctuations and defects induced by strain, which give rise to carrier localization. These effects<sup>11</sup> change the hole distribution in the energy levels and contribute to changes in the emission line shapes, mainly in the tails intensity strength of the PL spectra.

As an independent experimental verification of our interpretation, we also carried out PL measurements in the sample with  $x=0.51$  under an externally applied biaxial strain. To perform these experiments we used a pressure cell based on a plate bending method using a ring and a sphere.<sup>14–16</sup> The sample is fixed on the ring (see the inset of Fig. 4) and it is bent by pushing the sphere against the back side of the substrate. Using this procedure, a biaxial tensile strain is induced in the film. We used a 8 mm diameter ring and a sample dimension of  $1 \times 1$  cm<sup>2</sup>. The strain [defined as  $(a_{\text{strained}} - a_0)/a_0$ , where  $a_{\text{strained}}$  and  $a_0$  are lattice parameters of the externally strained and unstrained layer, respectively] is calibrated using the PL emission shift from the  $\text{In}_{0.53}\text{Ga}_{0.47}\text{As}$

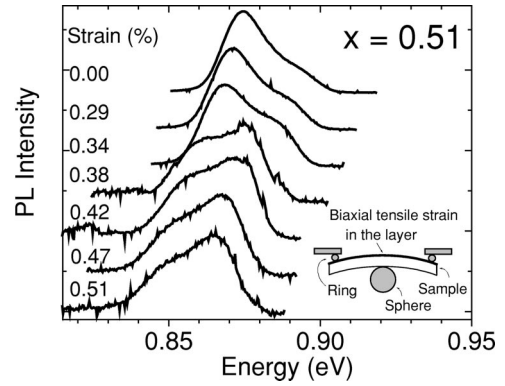


FIG. 4. Normalized photoluminescence spectra at 2 K for the sample with  $x=0.51$  under an external biaxial strain. The inset illustrates the scheme of the pressure cell.

buffer layer. The QW is located close to the buffer layer and the variation on the strain strength between these two layers is smaller than the experimental precision. The normalized PL spectra of this sample as a function of the external strain are shown in Fig. 4. There is a strong dependence of the PL line shape with the applied tensile strain. For low tensile strains the tail of the PL emission is located at the high-energy side of the spectrum. However, as the strain is increased the PL emission line shape changes and for high strain values, the tail appears at the low-energy side of the PL spectrum and the peak intensity decreases a factor  $\sim 3.5$ . The decreasing of the PL peak intensity is expected for the indirect band gap structure. The crossover of direct-indirect gap occurs for external strain between 0.34 and 0.38% (see Fig. 4). Assuming that the crossover strain is  $\sim 0.36\%$  the estimated value of the equivalent increasing Ga composition in the ternary alloy is  $\sim 0.05$ . Adding this value to the Ga composition of the sample it gives an alloy with  $x=0.56$ . It is in good agreement with the theoretical value,  $x=0.55$ . These results, therefore, are consistent with the theoretical prediction discussed above and unambiguously demonstrate the transition from direct-to-indirect gap in the same sample, driven solely by the biaxial strain.

#### IV. CONCLUSIONS

In conclusion, we presented experimental and theoretical evidence of the direct-to-indirect band gap structure transition in  $n$ -type modulation doped InGaAs/InP quantum wells using optical technique. PL measurements under externally applied tensile biaxial strain confirms the existence of direct-to-indirect band gap crossover.

#### ACKNOWLEDGMENTS

The authors gratefully acknowledge M. M. Tanabe for the technical support. This work was supported by CNPq, FINEP, and FAPESP.

- <sup>1</sup>D. Gershoni, J. M. Vandenberg, R. A. Hamm, H. Temkin, and M. B. Panish, *Phys. Rev. B* **36**, 1320 (1987).
- <sup>2</sup>D. Gershoni, H. Temkin, J. M. Vandenberg, S. N. G. Chu, R. A. Hamm, and M. B. Panish, *Phys. Rev. Lett.* **60**, 448 (1988).
- <sup>3</sup>D. Gershoni, H. Temkin, M. B. Panish, and R. A. Hamm, *Phys. Rev. B* **39**, 5531 (1989).
- <sup>4</sup>C. Y.-P. Chao and S. L. Chuang, *Phys. Rev. B* **46**, 4110 (1992).
- <sup>5</sup>M. Sugawara, N. Okazaki, T. Fujii, and S. Yamazaki, *Phys. Rev. B* **48**, 8102 (1993).
- <sup>6</sup>P. Michler, A. Hangleiter, A. Moritz, G. Fuchs, V. Härle, and F. Scholz, *Phys. Rev. B* **48**, 11 991 (1993).
- <sup>7</sup>A. L. C. Triques and J. A. Brum, *Proceedings of the 22nd International Conference on the Physics of Semiconductors, Vancouver, Canada, 1994*, edited by D. J. Lockwood (World Scientific, 1995), Vol. 2, pp. 1328–1331.
- <sup>8</sup>R. Weihofen, G. Weiser, Ch. Starck, and R. J. Simes, *Phys. Rev. B* **51**, 4296 (1995).
- <sup>9</sup>J. Dalfors, R. Lundström, P. O. Holtz, H. H. Radamson, B. Monemar, J. Wallin, and G. Landgren, *Appl. Phys. Lett.* **71**, 503 (1997).
- <sup>10</sup>T. J. C. Hosea and G. Rowland, *Supercond. Sci. Technol.* **13**, 207 (1998).
- <sup>11</sup>H. A. P. Tudury, E. Ribeiro, F. Iikawa, J. A. Brum, A. A. Bernussi, W. Carvalho, Jr., and A. Gobbi (unpublished).
- <sup>12</sup>G. Bastard and J. A. Brum, *IEEE J. Quantum Electron.* **22**, 1625 (1986).
- <sup>13</sup>G. Bastard, *Wave Mechanics Applied to Semiconductor Heterostructures* (Les Editions de Physique, Paris, 1992).
- <sup>14</sup>V. V. Baptizanskii, I. I. Novak, and Yu. F. Titovets, *Sov. Phys. Solid State* **21**, 1915 (1979).
- <sup>15</sup>E. Liarokapis and W. Richter, *Meas. Sci. Technol.* **3**, 347 (1992).
- <sup>16</sup>M. L. W. Thewalt, D. A. Harrison, C. F. Reinhart, J. A. Wolk, and H. Lafontaine, *Phys. Rev. Lett.* **79**, 269 (1997).